

Substitutions for Glutamate 101 in Subunit II of Cytochrome *c* Oxidase from *Rhodobacter sphaeroides* Result in Blocking the Proton-Conducting K-Channel[†]

Farol L. Tomson,[‡] Joel E. Morgan,[‡] Guoping Gu,^{‡,§} Blanca Barquera,[‡] T. V. Vygodina,^{||} and Robert B. Gennis^{*,‡}

Department of Biochemistry, University of Illinois, Urbana, Illinois 61801, and A. N. Belozersky Institute of Physico-Chemical Biology, Moscow State University, Moscow, Russia

Received August 27, 2002; Revised Manuscript Received December 12, 2002

ABSTRACT: Two functional input pathways for protons have been characterized in the heme–copper oxidases: the D-channel and the K-channel. These two proton-conducting channels have different functional roles and have been defined both by X-ray crystallography and by the characterization of site-directed mutants. Whereas the entrance of the D-channel is well-defined as D132^I (subunit I; *Rhodobacter sphaeroides* numbering), the entrance of the K-channel has not been clearly defined. Previous mutagenesis studies of the cytochrome *bo*₃ quinol oxidase from *Escherichia coli* implicated an almost fully conserved glutamic acid residue within subunit II as a likely candidate for the entrance of the K-channel. The current work examines the properties of mutants of this conserved glutamate in the oxidase from *R. sphaeroides* (E101^{II}I,A,C,Q,D,N,H) and residues in the immediate vicinity of E101^{II}. It is shown that virtually any substitution for E101^{II}, including E101^{II}D, strongly reduces oxidase turnover (to 8–29%). Furthermore, the low steady-state activity correlates with an inhibition of the rate of reduction of heme *a*₃ prior to the reaction with O₂. These are phenotypes expected of K-channel mutants. It is concluded that the predominant entry point for protons going into the K-channel of cytochrome oxidase is the surface-exposed glutamic acid E101^{II} in subunit II.

The heme–copper oxidases catalyze the reduction of dioxygen to water (1–3). In the process, four protons are consumed per O₂ to make two H₂O, and another four protons are pumped across the membrane.



The enzyme, thus, couples this chemical reaction to electrogenic movement of charge across the membrane, generating a proton motive force. Redox-active metal centers, Cu_A and heme *a*, provide the wire or pathway for electron transfer from the donor, ferrocycytochrome *c*, to the heme *a*₃–Cu_B binuclear center where the dioxygen chemistry is catalyzed. The binuclear center is buried within the protein, and the chemical reaction is, therefore, absolutely dependent upon pathways within the oxidase to facilitate proton diffusion from the bulk aqueous phase (bacterial cytoplasm or mitochondrial matrix) to the active site (4). Pathway(s) for pumped protons to get across to the bulk aqueous phase on the opposite side of the membrane (bacterial periplasm or

mitochondrial intermembrane space) must also be present (5).

X-ray structural models of bacterial oxidases and of the bovine mitochondrial cytochrome oxidase have indicated likely input proton-conducting pathways, leading from the surface of the protein to the vicinity of the heme–copper active site (4, 6–11, 12). The biochemical characterization of site-directed mutants has played a critical role in defining these pathways, which need not be evident from a purely structural analysis (3, 4, 13–22).

The D-channel is the most prominent of these pathways since it contains a chain of about a dozen water molecules in the X-ray structures, forming a hydrogen bond pathway from an aspartic acid (D132^I; *Rhodobacter sphaeroides* numbering¹, where the superscript indicates subunit I) to a buried glutamic acid (E286^I), which is about 10 Å from the active site. Mutations of either of these highly conserved acidic residues results in the elimination or dramatic reduction of the turnover rate. Site-directed mutagenesis studies prior to the determination of the X-ray structures suggested critical roles for both E286^I and D132^I in proton translocation (23–28). The pathway(s) for proton translocation beyond E286^I is uncertain and is likely to involve transient conformations and rearrangements of internal water molecules.

The K-channel is much less obvious from observation of the X-ray structures. The key residue is K362^I, which is

[†] Supported by grants from the National Institutes of Health HL16101 (R.B.G.), the Fogarty Foundation TW00349 (R.B.G. and A.A.K.), the U.S. Civilian Research and Development Foundation RC1-2063 (R.B.G. and A.A.K.), a NATO Collaborative Linkage Grant LST.CLG 975851 (R.B.G. and A.A.K.), Russian Fund for Basic Research 00-04-48262 (T.V.), and a Howard Hughes Medical Institute International Scholar Award 55000320 (A.A.K.).

* Corresponding author. Tel.: (217) 333-9075. Fax: (217) 244-3186. E-mail: r-gennis@uiuc.edu.

[‡] University of Illinois.

[§] Current address: Department of MCD Biology, 225 Sinsheimer Lab, University of California, Santa Cruz, CA 95064.

^{||} Moscow State University.

¹ The prominent residues referred to in this paper are indicated by the numbering in the *R. sphaeroides* oxidase: D132^I, E286^I, K362^I, S299^I (in subunit I), and E101^{II} in subunit II. These correspond to the following residues in the bovine oxidase: D91^I, E242^I, K319^I, S255^I, and E61^{II}.

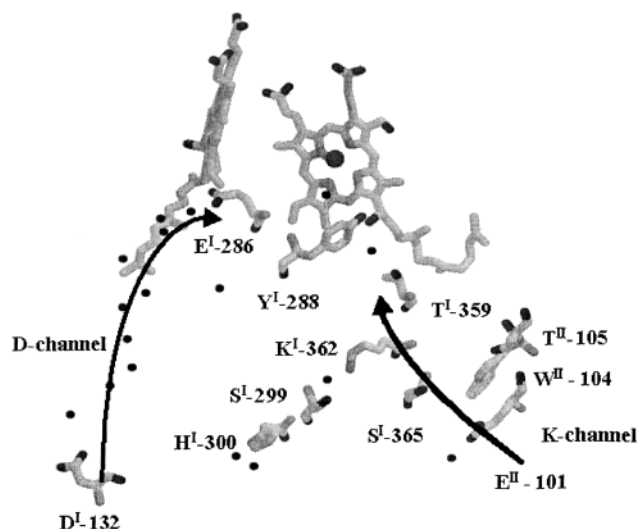


FIGURE 1: Model of the proton-conducting channels of cytochrome *c* oxidase, taken from the crystal structure of the *R. sphaeroides* oxidase (1M56) (12). The D-channel begins at D132^I and is connected to E286^I. The K-channel begins at E101^{II} and continues through K362^I past T359^I to the binuclear center. The amino acids studied in this paper are shown in relationship to the channels. The small black circles represent water molecules. The figure was prepared using RASMOL.

required for enzyme activity. This residue appears to have multiple roles, one of which is to facilitate proton diffusion to the binuclear center via a pathway that consists of a water molecule, the side chain of residue T359^I, and finally, Y288^I, which is at the active site and likely to be a direct participant in the catalytic function of the enzyme (13, 17, 20, 25, 29, 30). Unlike D132^I, this conserved lysine is buried within the protein. The current work is concerned with the pathway for protons leading from the surface of the enzyme to K362^I. Residues discussed are shown in Figure 1.

It had been proposed, based on the X-ray structures, that the pathway for protons to get to K362^I included S299^I and H300^I (see Figure 1) (8, 12). However, mutation of the equivalent residues in the oxidase from *Paracoccus denitrificans* did not result in any decrease in catalytic activity (22). It has also been shown that the mutation of S299^I in the *Escherichia coli* oxidase is benign (31). Recently, mutants in S299^I were examined in the *R. sphaeroides* oxidase (30). It was concluded that this residue is not involved in proton delivery to K362^I though it may be important to stabilize a protonated form of K362^I by hydrogen bonding to this residue through a bridging water molecule (30).

An alternate pathway leading to K362^I was first suggested by electrostatic calculations (32) indicating that the protonation state E101^{II} might depend on the redox state of the binuclear center, despite the rather long distance separating the two (about 25 Å). This residue is on the protein surface. E101^{II} is conserved to an extraordinary degree, being present in nearly all of the 1300 available sequences of subunit II. The functional importance of this residue was previously tested (31) by examining mutants of cytochrome *bo*₃ from *E. coli* (E89^{II}A,Q,D). These mutants all had impaired oxidase activity (43, 10, and 59%, respectively, for the A, Q, and D substitutions), consistent with a functional role for this glutamic acid. On the basis of the X-ray crystal structures, there are no other protonatable residues near K362^I that lead to the surface of the enzyme.

The phenotype of K-channel mutants is defined by the behavior of mutations K362^I and T359^I (13–15, 17, 29, 33–35) and can be summarized as follows: (1) Reduced rate of steady-state oxidase activity. (2) Impaired rate of reduction of the binuclear center prior to the interaction with O₂. The initial reduction of heme a₃/Cu_B by electron transfer from heme a requires the concomitant delivery of protons (one per electron) to the vicinity of the metals as a form of charge neutralization. K-channel mutants presumably impair this proton delivery, and hence, prevent or slow the coupled electron transfer. (3) Rapid reaction of O₂ with the fully reduced enzyme. The K-channel does not appear to be required for proton transfer during this reaction. However, K362 itself does play a role in facilitating the rate of formation of intermediate P_R (A → P_R step), apparently by a charge compensation mechanism requiring movement of the lysine side chain but not proton transfer (30). (4) Stimulation of turnover by using H₂O₂ in place of O₂ as an oxidant. The reaction with peroxide does not require prior reduction of the heme–copper center (blocked by K-channel mutants) since the substrate (peroxide) is itself two redox equivalents more reduced than O₂. Hydrogen peroxide essentially carries two electrons and two protons into the active site along with O₂ to form the initial oxygenated intermediate. (5) Impairment of the proton release associated with reverse electron transfer (backflow) from heme a₃ to heme a, which accompanies the photolysis of the CO adduct of the two-electron reduced (mixed-valence) form of the enzyme. This is conceptually the same process, although in the opposite direction as the proton uptake coupled to the reduction of heme a₃. Photolysis causes the expulsion of CO from the heme a₃ Fe, lowering the midpoint potential of the heme, and thus, resulting in oxidation of heme a₃ as the electrons redistribute to heme a and Cu_A. The proton release is pH-dependent (36–38) and is blocked in K-channel mutants (13).

In a preceding publication associated with the current work (39), it was shown that the E101^{II} mutants have impaired proton release in the backflow experiment and that the kinetics of the reaction of O₂ with the fully reduced enzyme (flow-flash reaction) are essentially the same as in the wild-type enzyme. The current work shows that the E101^{II} mutants have impaired steady-state turnover, and importantly, that the extent of inhibition of cytochrome oxidase activity correlates with the effects of the mutations on the rate of reduction of heme a₃ in the reaction of the oxidized enzyme with reductant. The E101^{II} mutants meet all the criteria as K-channel mutants. It is concluded that E101^{II} is part of the K-channel and is the predominant entry point for protons delivered to K362^I.

MATERIALS AND METHODS

Materials. Oligonucleotides used in cloning were obtained from the W. M. Keck Center for Comparative and Functional Genomics at the University of Illinois (Urbana, IL). The plasmids and strains used in the subunit II mutagenesis were gifts from Shelagh Ferguson-Miller and Yuejun Zhen (East Lansing, MI). Each of the mutants had a six-histidine tag at the end of subunit I to aid in purification (40). Hexaammineruthenium (III) chloride was purchased from Aldrich.

Amino Acid Alignment. The alignment program, Multalign (41), found at ch.embnet.org was used for amino acid

sequence comparisons. An alignment of subunit I (3427 entries) and subunit II (1354 entries) can be found at pfam.wustl.edu courtesy of Washington University (St. Louis, MO).

Mutagenesis. A modified version of the Kunkel method was used to create the site-directed mutants (42). The plasmids and protocol for the subunit II mutants were modified from that of Yuejun Zhen (43, 44). Sequencing was performed by the W. M. Keck Center for Comparative and Functional Genomics at the University of Illinois (Urbana, IL) to confirm each mutation.

Cell Growth and Protein Purification. Growth and purification of his-tagged mutants was according to Mitchell and Gennis (40). The protein used for the reduction kinetics assays was further purified by means of a DEAE column (44) using Toyopearl DEAE-650S (Tosoh Biosep, Montgomeryville, PA). The enzyme, after binding to the column, was washed with 100 mM KCl, 100 mM Tricine (pH 8.0), and 0.1% dodecyl- β -D-maltoside (DM)² and then eluted with the same buffer supplemented with 200 mM KCl. The KCl was removed by dialysis prior to use.

Cytochrome Oxidase Activity. Cytochrome *c* oxidase activity was measured spectroscopically by following the initial rate of oxidation of horse heart ferrocyanochrome *c* at 550 nm using a Shimadzu UV-2101PC spectrometer. The reaction medium contained 50 mM potassium phosphate, pH 6.5, 0.02% DM, and 2–50 μ M ferrocyanochrome *c*.

UV–Vis Steady-State Spectroscopy. UV–vis spectroscopy was performed with a Shimadzu UV-2101PC spectrometer. The buffer contained 100 mM potassium phosphate (pH 8.0), 0.1% DM, 0.2 mM ferricyanide, 56 μ g/mL poly-L-lysine, and 1 μ M enzyme. After the initial oxidized spectrum was taken, 30 mM ascorbate and 30 μ M TMPD were added to initiate turnover. Spectra were taken every 2 min for 10 min. To fully reduce the enzyme, a few grains of solid dithionite were added after 10 min, after which a reduced spectrum was recorded.

Peroxidase Activity. Ferrocyanide peroxidase assays were performed using the protocol of Vygodina et al. (29). Measurements were carried out with a DW2000 UV–vis spectrometer (SLM Instruments, Inc.) in dual wavelength mode. The accumulation of ferricyanide was measured by the absorbance difference $A_{420\text{ nm}} - A_{500\text{ nm}}$. The buffer contained 50 mM MOPS–KOH (pH 7.0), 0.5 mM EDTA, 40 μ g/mL poly-L-lysine, 0.1% DM, 10 mM imidazole, 0.5 μ M enzyme, 0.5 μ M horse heart cytochrome *c*, and 1 mM ferricyanide. During the course of the experiment, 0.1 mM ferrocyanide, 4 mM H₂O₂, and 4 mM KCN were added. The concentrations of ferricyanide and ferrocyanide were varied from sample to sample to obtain a flat baseline ($A_{420-500}$ vs time). In a few cases, it was necessary to record the changes in the slope of the baseline prior to the additions and subtract to adjust the time-course data.

Measuring the Rate of Reduction of Heme *a*₃. Measurements of the rate of reduction of heme *a*₃ were carried out using a method based on the work of Verkhovsky et al. (45) using hexaammineruthenium (III) as the reductant. Since fully oxidized cytochrome oxidase can convert to a less active resting form that has properties distinct from the form

engaged in turnover, it is necessary to pulse the enzyme just prior to use (45, 46). This requires that the enzyme be reduced and then reoxidized just prior to study. The goal is to obtain a homogeneous population of active oxidized (pulsed) enzyme. To accomplish this, the enzyme is first fully reduced in the presence of excess reductant (hexaammineruthenium plus dithionite). Using a stopped-flow spectrophotometer, the enzyme is then mixed with buffer containing O₂. Upon mixing, the O₂ oxidizes the enzyme within the dead-time of the instrument, leaving it in an active oxidized (pulsed) state. The excess dithionite removes the remaining oxygen very rapidly leaving the enzyme to be rereduced by the hexaammineruthenium.

Rereduction kinetics were monitored spectroscopically using an Applied Photophysics SX-18MV stopped-flow spectrophotometer (Leatherhead, U.K.) equipped with a photodiode array (PDA) detector. The instrument was maintained at 20 °C by means of a circulating water bath. Hexaammineruthenium (III) was used as an electron donor. As a loading reservoir, a 5-mL Hamilton series C syringe was attached to the thread at one of the loading ports of the stopped-flow unit; because of the depth of the port, the cylindrical kel-F seal in the end of the syringe was replaced by a slightly longer cylinder to ensure a good seal. A total of 10 μ M enzyme was added to a buffer containing 100 mM tricine (pH 8.0) and 0.1% DM and placed in this reservoir. The sample was made air free by directing a gentle jet of water-saturated nitrogen or argon gas into the liquid surface. A total of 10 mM hexaammineruthenium was then added together with 40 mM dithionite as reductant, and the sample was loaded into one of the driving syringes. Air-saturated buffer (\sim 250 μ M O₂) was then loaded into the second driving syringe.

Upon mixing, the oxidation of the enzyme and reduction of heme *a* are both essentially complete within the dead-time of the instrument. The excess dithionite rapidly removes any O₂ remaining in solution, and reduction of heme *a*₃ takes place in the absence of O₂. After mixing, spectra were acquired using the PDA every 2.56 ms for 2 or 4 s. In the resulting data surface, wavelength points are spaced 3.3 nm apart. The data were processed using MATLAB (The Mathworks, South Natick, MA), and a global multiexponential fit was carried out using SPLMOD (47).

RESULTS

The targeted E101^{II} residue is part of a cluster of residues near the cytoplasmic end of a transmembrane helix: E101^{II}IAWTIVP¹⁰⁸. The E101 residue is nearly 100% conserved. Several other residues within the cluster are also significantly conserved, although to a much lesser extent than E101^{II}. The P108^{II} residue, which is in contact with the farnesyl side chain of heme *a*, is the next most highly conserved in this cluster. To test the hypothesis that E101^{II} is functionally part of the K-channel, the following seven mutational substitutions were made: E101^{II}I,A,C,Q,D,N,H. In addition, mutations were made in several nearby residues to examine the general effects of perturbations to this region: W104^{II}V, T105^{II}A, and L100^{II}A. Finally, since S299^I and H300^I have been previously suggested as being at the entry to the K-channel (8), mutations were also made in these positions: S299^IA and H300^IA.

² Abbreviations: DM, dodecyl- β -D-maltoside.

Table 1: Cytochrome *c* Oxidase Activities of the Mutants

	cyt <i>c</i> oxidase activity turnover (s ⁻¹)	relative oxidase activity	ferrocyanide peroxidase activity	rate of reduction of heme a ₃ (s ⁻¹)
WT	1452	100	Y	159
H300 ^I A	1606	111	Y	149
S299 ^I A	660	45	N	139
K362 ^I M	<5	0	Y	ND
E101 ^{II} I	120	8	Y	4
E101 ^{II} A	122	8	Y	5
E101 ^{II} C	132	8	Y	1
E101 ^{II} Q	207	14	Y	2
E101 ^{II} D	232	16	Y	5
E101 ^{II} N	251	17	Y	2
E101 ^{II} H	427	29	Y	15
W104 ^{II} V	659	45	Y	54
T105 ^{II} A	728	50	Y	80
L100 ^{II} A	2133	147	Y	131

Each mutant oxidase was purified and characterized. In all cases, the UV-vis spectra of the ferricyanide-oxidized and dithionite-reduced forms of the enzymes are essentially identical to those of the wild-type control (not shown). The cytochrome *c* oxidase activity of each mutant was also measured, and the results are summarized in Table 1. The most dramatic effects are the low activities of each of the seven mutations at E101^{II}. Replacement of this glutamate by the hydrophobic residues isoleucine, cysteine, or alanine reduced the turnover to about 8% that of the wild-type control. The glutamine, aspartate, and asparagine substitutions led to about 16% of wild-type activity. The histidine mutant had the highest activity of the set, 29% as compared to the wild type. The other mutants were considerably more active. The L100^{II}A and H300^IA had specific activities close to that of the wild-type control. The remaining mutants, S299^IA, W104^{II}V, and T105^{II}A, had approximately 45% of wild-type activity. These data are consistent with a unique functional role for E101^{II} and provide further evidence that H300^I in subunit I is not at the entrance of the K-channel (22).

One of the characteristics of K-channel mutants is that they retain the ability to use hydrogen peroxide as an oxidant (15, 29). Reaction with O₂ is blocked because the reduction of the heme-copper center is inhibited, but H₂O₂ can react directly with the fully oxidized enzyme to form species P, and the K-channel mutations appear not to block the steps after this in the catalytic cycle. One way to measure the peroxidase activity, specifically using this pathway (i.e., reaction of H₂O₂ with the fully oxidized enzyme), is by using a high-potential reductant such as ferrocyanide (29), which cannot reduce ferric heme a₃ but can readily donate an electron to the oxoferryl species P and F. Figure 2 shows that the behavior of the E101^{II}C mutant is similar to that of K362^IM (i.e., E101^{II}C has ferrocyanide peroxidase activity). Qualitatively, at least, the E101^{II}C mutant has a functional D-channel since ferrocyanide peroxidase reaction requires the D-channel (29). An unexpected finding is that S299^IA does not exhibit this peroxidase activity. The reason for this is not known but may be related to the functions postulated for K362^I other than proton delivery that are perturbed by mutations in S299^I (30).

If the E101^{II} mutations effectively block the K-channel, then it is expected that the rate of reduction of ferric heme a₃ via heme a should be slowed as compared to the wild-

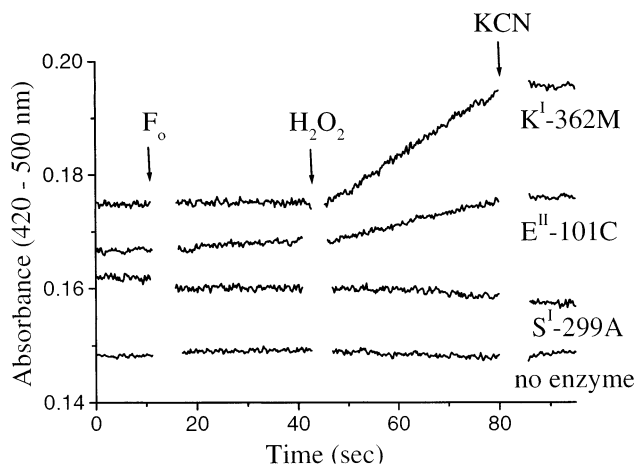


FIGURE 2: Ferrocyanide peroxidase activity assay for K362^IM, E101^{II}C, S299^IA, and a control with no enzyme present. The initial buffer contained 50 mM MOPS-KOH (pH 7.0), 0.5 mM EDTA, 40 μ g/mL poly-L-lysine, 0.1% DM, 10 mM imidazole, 0.5 μ M enzyme, 0.5 μ M horse heart cytochrome *c*, and approximately 1 mM ferricyanide. Additions of the following were made at times indicated by the arrows: approximately 0.1 mM ferrocyanide (F₀), 4 mM H₂O₂, and 4 mM KCN.

type enzyme (29). If the E101^{II} mutations selectively block the heme a \rightarrow heme a₃ electron-transfer step in the catalytic cycle, the expected consequence would be a greater extent of reduction of heme a during steady-state turnover. This is observed. Figure 3 shows spectra taken during the steady-state turnover of the enzyme. In this experiment, ascorbate/TMPD is used as the reductant. Since TMPD does not donate electrons to the enzyme efficiently, the reaction is slow. Wild-type enzyme under these conditions takes more than 10 min to deplete the O₂ in the cuvette and become fully reduced. Spectra were recorded during this period, after which dithionite was added to complete the reduction of the enzyme. Results are shown for the wild type and for the E101^{II}C mutant. All spectra shown are difference spectra with the fully oxidized enzyme as the reference. The extent of reduction of heme a is evaluated by the height of the absorbance peak at 606 nm. During turnover with ascorbate/TMPD, the extent of reduction of heme a in the mutant is 67%, as compared to only 32% for the wild-type enzyme under the same conditions. A similar effect is observed with the other E101^{II} mutants (not shown).

The reduction of heme a₃ can be directly measured at 445 nm using a stopped-flow spectrophotometer. Representative data are shown in Figure 4, and the calculated first-order rate constants are contained in Table 1. The rates were obtained from a two-exponential fit to the entire multiwavelength surface as described in the Materials and Methods section. The predominant phase is associated with spectroscopic changes that correspond to ferrous – ferric heme a₃ (Figure 4, inset).

Under the experimental conditions used, the reduction of heme a₃ in the wild-type enzyme is complete in less than 0.1 s ($k = 159$ s⁻¹). The E101^{II} mutants all have substantially slower rates of reduction of heme a₃, with the slowest being E101^{II}C, which takes over 4 s to reduce completely and has a first-order rate constant of 0.6 s⁻¹.

Figure 5 shows a correlation between the rates obtained for the reduction of heme a₃ in these experiments and the turnover rates obtained in the standard cytochrome *c* oxidase

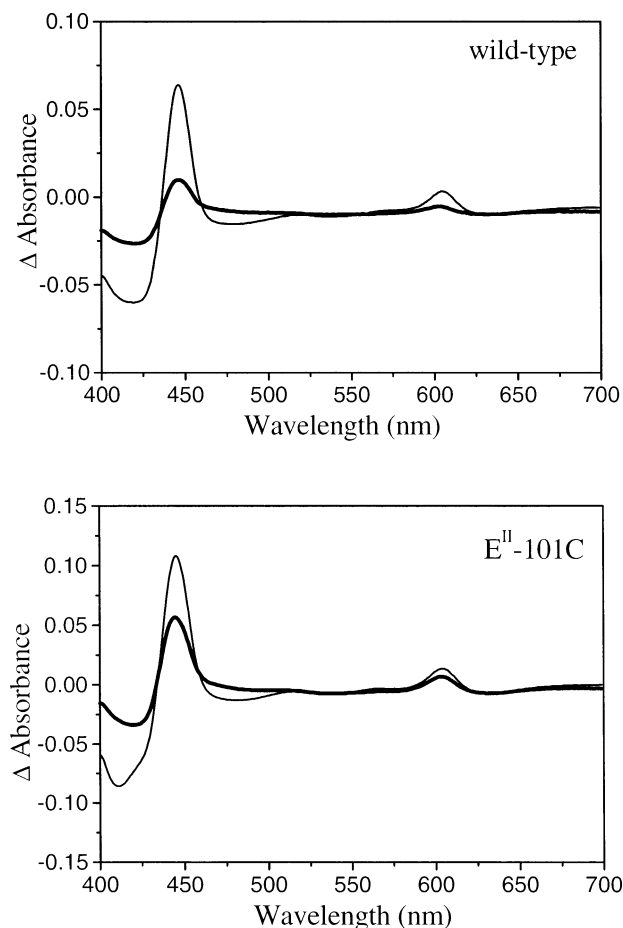


FIGURE 3: Spectra of wild-type and E101^{II}C cytochrome *c* oxidases during steady-state turnover. The difference spectra of the fully (dithionite) reduced minus ferricyanide oxidized enzymes are shown (thin line), along with the difference spectra showing the steady state minus ferricyanide oxidized enzymes. Samples contained 1 μ M enzyme in 100 mM potassium phosphate (pH 8.0), and 0.1% DM. The enzyme was oxidized by 0.2 mM ferricyanide and 56 μ g/mL poly-L-lysine. After the initial spectrum of the oxidized enzyme was taken, 30 mM ascorbate and 30 μ M TMPD (*N,N,N',N'*-tetramethyl-*p*-phenylenediamine) were added to initiate enzyme turnover. Spectra were taken every 2 min for 10 min. The steady-state spectrum used in the figure is that obtained at the 4 min time point. A few grains of solid dithionite were added after 10 min to fully reduce the enzyme before a final spectrum was taken.

assay. There is clearly a qualitative correlation between these measurements, suggesting that the primary reason for the reduced steady-state turnover is the slow rate of reduction of ferric heme *a*₃. This is the primary feature of K-channel mutants. These data strongly support the hypothesis that E101^{II} is the main entry point for protons into the K-channel.

DISCUSSION

All of the data presented in this work are consistent with the assignment of E101^{II} to the entrance to the K-channel. Currently, more than 1300 heme–copper oxidase subunit II sequences are available. Only three of these do not have an equivalent of E101^{II}: *Forficula lesnei* (earwig) contains a lysine at this position (48). *Rhagoletotrypeta pastranai* (fly) contains an aspartate (49), and a sequence fragment from *Otholobium sericeum* (legume) contains a glycine (50). Glutamate is present in all the other sequences, attesting to the importance of this residue. In the X-ray structural models of both the bovine (9) and the *P. denitrificans* oxidases (10,

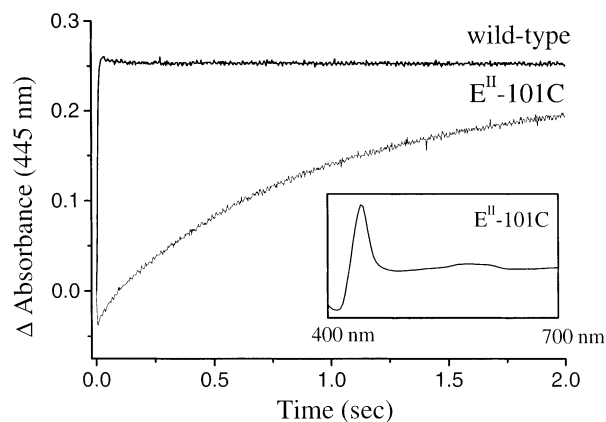


FIGURE 4: Kinetics of reduction of the wild type and E101^{II}C cytochrome *c* oxidases from *R. sphaeroides*. The reduction of heme *a*₃ by hexaammineruthenium was monitored at 445 nm for 2 s. The experiment was performed in a stopped-flow instrument where one syringe contained air-saturated buffer (256 μ M oxygen) of 100 mM Tricine, pH 8.0, and 0.1% DM. The other syringe contained an anaerobic solution of 10 μ M enzyme, 40 mM dithionite, and 10 mM hexaammineruthenium (III) chloride in the same buffer. The data are fit to two kinetic phases, with the larger phase accounting for about 99% of the amplitude. The insert is the 400–700 nm optical spectrum of the major kinetic phase of the E101^{II}C oxidase, and this spectrum corresponds to the ferrous minus ferric difference spectrum of heme *a*₃ (45). The reduction of heme *a* occurs within the dead-time of the instrument.

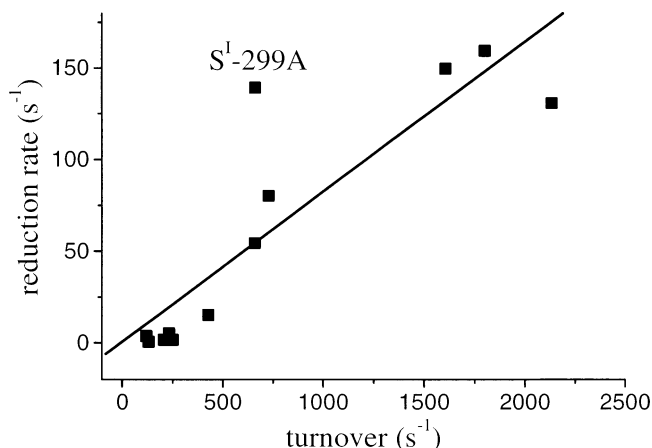


FIGURE 5: Comparison between cytochrome *c* oxidase steady-state turnover activity and the first-order apparent rate constant for reduction of heme *a*₃ by hexaammineruthenium (III). The correlation between the two rates suggests that the primary reason for the reduced steady-state turnover is the slow rate of reduction of ferric heme *a*₃. The outlying data point is due to S299^IA, which is concluded not to be in the proton-conducting pathway. The numerical values are given in Table 1.

11), this glutamate is on the surface of the enzyme, and the carboxyl moiety is not hydrogen bonded to any another residue. It is clear from the sequence alignments that glutamate is specifically required at this position and that even aspartate is not an equivalent substitute. This is demonstrated by the current work. The E101^{II}D mutant has only 13% of the activity of the wild-type oxidase, and the rate constant for reduction of heme *a*₃ is only 5 s⁻¹, as compared to about 159 s⁻¹ for the wild-type enzyme under the experimental conditions examined.

The rate of reduction of heme *a*₃ is coupled to, and limited by, proton transfer, presumably to a group in the vicinity of the binuclear center and also depends on the redox driving

force of the reductant (45). There is a rapid equilibrium of the electrons among the metal centers in the enzyme. Initially, this equilibrium strongly disfavors reduction of heme a_3 , but proton transfer to the active site shifts the equilibrium to favor reduced heme a_3 . The rate of accumulation of reduced heme a_3 depends on both the rate constant for proton transfer and on the population of enzyme, which has reduced heme a_3 and an available protonation site (45). The simplest interpretation of the current data is that the E101^{II} mutations limit the rate by which protons are delivered to the active site through the K-channel, and thus, limit the rate of accumulation of reduced heme a_3 . The fact that the E101D^{II} mutant has a much lower activity than the wild-type oxidase indicates that the role of the glutamic acid at this position is not simply electrostatic. There must be a specific structural requirement fulfilled by E101^{II} for optimal proton uptake into the K-channel. The effect of substitutions for W104^{II} and T105^{II} must be due to a structural perturbation in the region of the protein around E101^{II}.

The current results are consistent with previous observations. Mutations of the equivalent glutamate in *E. coli* cytochrome bo_3 (E89^{II}) also reduce catalytic turnover (31). In the case of the *E. coli* enzyme, placing an aspartate at this position is much less damaging than it is in the *R. sphaeroides* oxidase. The E89^{II}D mutation is 59% active as compared to the wild type, and even the E89^{II}A mutant is 43% active. By contrast, E89^{II}Q is only 10% active, similar to the effect of the E101^{II}Q mutant reported in the current work. It may be significant that none of the mutations in either the *E. coli* or the *R. sphaeroides* oxidases result in complete elimination of catalytic turnover, indicating alternate pathways for proton entry to the K-channel. The fact that the effects of mutations at this site depend to some extent on the particular oxidase being examined may reflect variations in proton-conducting pathways.

Neither the S299^I or H300^I residues are required for proton delivery through the K-channel (Table 1), confirming previous studies with the *P. denitrificans* oxidase (22). A different function for S299^I was demonstrated in earlier studies of the *R. sphaeroides* oxidase. The S299^IG and S299^ID mutations slow the rate of formation of species P_R in the single-turnover reaction of O_2 with the fully reduced enzyme (30). This has been interpreted to mean that S299^I, through an interaction with a bridging water molecule, stabilizes a protonated form of K362^I and that movement of this cationic side chain facilitates charge transfer during the formation of P_R .

With the identification of E101^{II} as the entrance of the K-channel, each of the two proton input channels of the oxidase (i.e., the D-channel and the K-channel) has an acidic group at its entry point. The entrance to the D-channel is D132^I, which is near the surface of the enzyme, although not as exposed as E101^{II} (7, 8, 10, 11). Mutations of D132^I (to A or N) drastically reduce steady-state turnover (<5%) (17, 27, 51, 52). In these D-channel mutants, however, the rate of reduction of ferric heme a_3 is not altered, but some steps in the reaction of the fully reduced enzyme with O_2 are strongly inhibited.

It has been suggested that the K-channel may not actually conduct protons but functions, instead, as a dielectric well, such that charge rearrangements within the channel lower the energy barrier for internal charge transfers involved in the reduction of the binuclear center (53). Indeed, the

explanation of the effect of the S299^I mutations on the rate of formation of P_R invokes this mechanism (30). However, the E101^{II} mutations do not inhibit the rate of P_R formation. The dramatic influence on both steady-state turnover and on the rate of reduction of heme a_3 because of mutations of E101^{II}, which is exposed on the protein surface, is difficult to rationalize as being due to a dielectric well phenomenon. Furthermore, it has been demonstrated that the K-channel is necessary for proton release into solution upon oxidation of heme a_3 during reverse electron transfer (13), and the E101^{II} mutations dramatically slow this proton release (39). Although the K-channel does not have a chain of water molecules that nicely delineates a proton-conducting pathway, the experimental evidence strongly suggests that the K-channel facilitates net proton diffusion to/from the enzyme active site.

The current work also indicates that the K-channel does not contain a bound proton that can be readily delivered to the enzyme active site without concomitant proton uptake from solution, at least under the rereduction conditions utilized. Blocking the K-channel at the entrance (e.g., E101^{II}C) drastically slows down the reduction of heme a_3 (Table 1). Hence, proton delivery to the active site appears to be closely coupled to proton uptake from solution. This result is quite different from what has been observed with the D132^I mutants that block the entrance of the D-channel (51). In this case, there is an internal proton, presumably on E286^I, that can be rapidly delivered to the enzyme active site even in the absence of proton uptake in the D132^I mutants. This available proton allows the reaction of the fully reduced enzyme with O_2 to proceed to form compound F, even in the absence of proton uptake from solution. Since this internal proton cannot be replaced in the D132^I mutants, the reaction can proceed no further than the formation of compound F.

In summary, subunit II of cytochrome oxidase has two functional roles during catalytic turnover. Subunit II plays a critical role not only as an entry point for electrons, via Cu_A (1), but also as an entry point for protons via the K-channel.

ACKNOWLEDGMENT

Many thanks to Yuejun Zhen for a copy of his thesis and for all the plasmids and strains he provided. Many thanks also to S. Iwata for providing the *R. sphaeroides* coordinates.

REFERENCES

1. Ferguson-Miller, S., and Babcock, G. T. (1996) *Chem. Rev.* 7, 2889–2907.
2. Michel, H. (1999) *Biochemistry* 38, 15129–15140.
3. Zaslavsky, D., and Gennis, R. B. (2000) *Biochim. Biophys. Acta* 1458, 164–179.
4. Gennis, R. B. (1998) *Biochim. Biophys. Acta* 1365, 241–248.
5. Puustinen, A., and Wikström, M. (1999) *Proc. Natl. Acad. Sci. U.S.A.* 96, 35–37.
6. Yoshikawa, S., Shinzawa-Itoh, K., and Tsukihara, T. (2000) *J. Inorg. Biochem.* 82, 1–7.
7. Yoshikawa, S., Shinzawa-Itoh, K., Nakashima, R., Yaono, R., Yamashita, E., Inoue, N., Yao, M., Fei, M. J., Libeu, C. P., Mizushima, T., Yamaguchi, H., Tomizaki, T., and Tsukihara, T. (1998) *Science* 280, 1723–1729.
8. Tsukihara, T., Aoyama, H., Yamashita, E., Takashi, T., Yamaguchi, H., Shinzawa-Itoh, K., Nakashima, R., Yaono, R., and Yoshikawa, S. (1996) *Science* 272, 1136–1144.

9. Tsukihara, T., Aoyama, H., Yamashita, E., Tomizaki, T., Yamaguchi, H., Shinzawa-Itoh, K., Nakashima, T., Yaono, R., and Yoshikawa, S. (1995) *Science* 269, 1069–1074.
10. Iwata, S., Ostermeier, C., Ludwig, B., and Michel, H. (1995) *Nature* 376, 660–669.
11. Ostermeier, C., Harrenga, A., Ermler, U., and Michel, H. (1997) *Proc. Natl. Acad. Sci. U.S.A.* 94, 10547–10553.
12. Svensson-Ek, M., Abramson, J., Larsson, G., Tornroth, S., Brzezinski, P., and Iwata, S. (2002) *J. Mol. Biol.* 321, 329–39.
13. Ådelroth, P., Gennis, R. B., and Brzezinski, P. (1998) *Biochemistry* 37, 2470–2476.
14. Ådelroth, P., Gennis, R. B., and Brzezinski, P. (1998) *Biochemistry* 37, 3062–3067.
15. Zaslavsky, D., and Gennis, R. B. (1998) *Biochemistry* 37, 3062–3067.
16. Ådelroth, P., Ek, M. S., Mitchell, D. M., Gennis, R. B., and Brzezinski, P. (1997) *Biochemistry* 36, 13824–13829.
17. Konstantinov, A. A., Siletsky, S., Mitchell, D., Kaulen, A., and Gennis, R. B. (1997) *Proc. Natl. Acad. Sci. U.S.A.* 94, 9085–9090.
18. Mitchell, D. M., Fetter, J. R., Mills, D. A., Ådelroth, P., Pressler, M. A., Kim, Y., Aasa, R., Brzezinski, P., Malmström, B. G., Alben, J. O., Babcock, G. T., Ferguson-Miller, S., and Gennis, R. B. (1996) *Biochemistry* 35, 13089–13093.
19. Vygodina, T., Mitchell, D., Pecoraro, C., Gennis, R., and Konstantinov, A. (1996) *EBEC Reports* 9, 93.
20. Hosler, J. P., Shapleigh, J. P., Mitchell, D. M., Kim, Y., Pressler, M., Georgiou, C., Babcock, G. T., Alben, J. O., Ferguson-Miller, S., and Gennis, R. B. (1996) *Biochemistry* 35, 10776–10783.
21. Pfützner, U., Hoffmeier, K., Harrenga, A., Kannt, A., Michel, H., Bamberg, E., Richter, O.-M. H., and Ludwig, B. (2000) *Biochemistry* 39, 6756–6762.
22. Pfützner, U., Odenwald, A., Ostermann, T., Weingard, L., Ludwig, B., and Richter, O.-M. H. (1998) *J. Bioenerg. Biomembr.* 30, 89–93.
23. Hosler, J. P., Ferguson-Miller, S., Calhoun, M. W., Thomas, J. W., Hill, J., Lemieux, L., Ma, J., Georgiou, C., Fetter, J., Shapleigh, J., Tecklenburg, M. M. J., Babcock, G. T., and Gennis, R. B. (1993) *J. Bioenerg. Biomembr.* 25, 121–136.
24. Thomas, J. W., Puustinen, A., Alben, J. O., Gennis, R. B., and Wikström, M. (1993) *Biochemistry* 32, 10923–10928.
25. Thomas, J. W., Lemieux, L. J., Alben, J. O., and Gennis, R. B. (1993) *Biochemistry* 32, 11173–11180.
26. Thomas, J. W., Calhoun, M. W., Lemieux, L. J., Puustinen, A., Wikström, M., Alben, J. O., and Gennis, R. B. (1994) *Biochemistry* 33, 13013–13021.
27. Fetter, J. R., Qian, J., Shapleigh, J., Thomas, J. W., Garcia-Horsman, A., Schmidt, E., Hosler, J., Babcock, G. T., Gennis, R. B., and Ferguson-Miller, S. (1995) *Proc. Natl. Acad. Sci. U.S.A.* 92, 1604–1608.
28. Garcia-Horsman, J. A., Puustinen, A., Gennis, R. B., and Wikström, M. (1995) *Biochemistry* 34, 4428–4433.
29. Vygodina, T. V., Pecoraro, C., Mitchell, D., Gennis, R., and Konstantinov, A. A. (1998) *Biochemistry* 37, 3053–3061.
30. Brändén, M., Sigurdson, H., Namslauer, A., Gennis, R. B., Ådelroth, P., and Brzezinski, P. (2001) *PNAS* 98, 5013–5018.
31. Ma, J., Tsatsos, P. H., Zaslavsky, D., Barquera, B., Thomas, J. W., Katsonouri, A., Puustinen, A., Wikström, M., Brzezinski, P., Alben, J. O., and Gennis, R. B. (1999) *Biochemistry* 38, 15150–15156.
32. Kannt, A., Lancaster, C. R. D., and Michel, H. (1998) *Biophys. J.* 74, 708–721.
33. Ruitenber, M., Kannt, A., Bamberg, E., Ludwig, B., Michel, H., and Fendler, K. (2000) *PNAS* 97, 4632–4636.
34. Verkhovsky, M. I., Tuukkanen, A., Backgren, C., Puustinen, A., and Wikström, M. (2001) *Biochemistry* 40, 7077–7083.
35. Wikström, M., Jasaitis, A., Backgren, C., Puustinen, A., and Verkhovsky, M. I. (2000) *Biochim. Biophys. Acta* 1459, 514–520.
36. Brzezinski, P. (1996) *Biochemistry* 35, 5611–5615.
37. Ådelroth, P., Brzezinski, P., and Malmström, B. G. (1995) *Biochemistry* 34, 2844–2849.
38. Hallén, S., Brzezinski, P., and Malmström, B. G. (1994) *Biochemistry* 33, 1467–1472.
39. Brändén, M., Tomson, F. L., Gennis, R. B., and Brzezinski, P. (2002) *Biochemistry* 41, 10794–10798.
40. Mitchell, D. M., and Gennis, R. B. (1995) *FEBS Lett.* 368, 148–150.
41. Corpet, F. (1988) *Nucleic Acids Res.* 16, 10881–10890.
42. Kunkel, T. A., Bebenek, K., and McClary, J. (1991) *Methods Enzymol.* 204, 125–139.
43. Zhen, Y., Schmidt, B., Kang, U. G., Antholine, W. E., and Ferguson-Miller, S. (2002) *Biochemistry* 41, 2288–2297.
44. Zhen, Y., Qian, J., Follmann, K., Hayward, T., Nilsson, T., Dahn, M., Hilmi, Y., and Hamer, A. G. (1998) *Protein Expr. Purif.* 13, 326–336.
45. Verkhovsky, M. I., Morgan, J. E., and Wikström, M. (1995) *Biochemistry* 34, 7483–7491.
46. Moody, A. J. (1996) *Biochim. Biophys. Acta* 1276, 6–20.
47. Provincer, S. W., and Vogel, R. H. (1983) *Prog. Sci. Comput.* 2, 304–319.
48. Wirth, T., LeGuellec, R., and Veuille, M. (1999) *Mol. Biol. Evol.* 16, 1645–1653.
49. Smith, J. J., and Bush, G. L. (1997) *Mol. Phylogenet. Evol.* 7, 33–43.
50. Adams, K. L., Song, K., Roessler, P. G., Nugent, J. M., Doyle, J. L., Doyle, J. J., and Palmer, J. D. (1999) *Proc. Natl. Acad. Sci. U.S.A.* 96, 13863–13868.
51. Smirnova, I. A., Ådelroth, P., Gennis, R. B., and Brzezinski, P. (1999) *Biochemistry* 38, 6826–6833.
52. Fetter, J., Sharpe, M., Qian, J., Mills, D., Ferguson-Miller, S., and Nicholls, P. (1996) *FEBS Lett.* 393, 155–160.
53. Jünemann, S., Meunier, B., Gennis, R. B., and Rich, P. R. (1997) *Biochemistry* 36, 14456–14464.

BI026750Y